

Arrays of self-sealed microchambers and channels

Mary Seto,^{*a} Ken Westra^b and Michael Brett^a

^aDepartment of Electrical and Computer Engineering, University of Alberta, Edmonton, AB, Canada T6G 2V4. E-mail: seto@ee.ualberta.ca

^bUniversity of Alberta NanoFab, University of Alberta, Edmonton, AB, Canada T6G 2V4

Received 13th March 2002, Accepted 11th June 2002

First published as an Advance Article on the web 27th June 2002

Arrays of self-sealed structures have been grown on silicon mesas and lines, which consist of porous thin film centres enclosed by solid borders, and can be fabricated in a single step using a unique method of film growth called glancing angle deposition (GLAD). These specialized structures may have potential for use in microreactor, microfluidic, chromatographic, nano-assay, lab-on-a-chip, biochemical, and other related applications.

Introduction

Advancements in miniaturized systems and lab-on-a-chip testing apparatus have rapidly progressed as the need for fast, inexpensive, and efficient testing methods and analytical tools has increased. In the past two decades, the biological and medical fields have seen great advances in the development of biosensors and biochips capable of performing various tasks.¹ Compared with traditional analytical instruments, chip-sized microsystems offer many advantages, from small dimensions, which give freedom from spatial limitations, to lower consumption of reagents and energy, which mean savings in cost and more efficient usage of resources.² The unique structures that have been developed here may offer applications in these areas.

Experimental and results

Silicon mesas and channels were fabricated using the Bosch Deep Silicon Reactive Ion Etch³ process in an Oxford PlasmaLab 100 inductively coupled plasma reactive ion etcher (ICP RIE) system. The mesas and channels were masked during the deep Si etch by a thermal oxide mask, which was formed by placing 100 mm diameter silicon wafers into a furnace at 950 °C. Injecting steam into the furnace during the oxidation formed an oxidizing environment that resulted in a 0.6 µm thick thermal oxide layer. The desired pattern of mesas and lines was then transferred to the oxidized silicon wafers by standard photolithography,⁴ after which a 10:1 buffered oxide etching (BOE) solution was used to remove the thermal oxide. The remaining photoresist was then removed after this wet etch step using an acetone wash. Finally, the wafer was placed in the ICP RIE, where the Bosch process was used to etch the structures to a depth of 14 µm. Three different arrays of mesas having square faces measuring approximately 2.5 × 2.5 µm, 7 × 7 µm, and 25 × 25 µm were utilized for subsequent deposition of the microchamber wells. The smallest of the mesas is shown in Fig. 1. The scalloped profile of the Si mesas is an artifact of the Bosch etch process.³ An areal view of the mesas (after a film has been deposited on them) can be seen in Fig. 4, and the Si lines, which varied in width, ranging from 2.5 to 50 µm, are shown in Fig. 2.

The GLAD technique was utilized to fabricate the self-sealed microchamber compartments surmounting the mesas. Porous, columnar thin films with engineered microstructures can be fabricated using this technique,^{5–7} with two predominant growth processes, namely enhanced shadowing and limited adatom diffusion, governing film growth under high vacuum

conditions. As the name of this technique implies, the substrates are oriented at highly oblique (or glancing) angles to the source material (typically, $\alpha > 80^\circ$, see Fig. 3). This causes the shadowing effect to become greatly enhanced, as vapour atoms arriving from the source to the substrate nucleate and create sites of preferential growth for additional film material. These areas then physically shadow regions of the substrate behind them. Since the substrates are not heated,

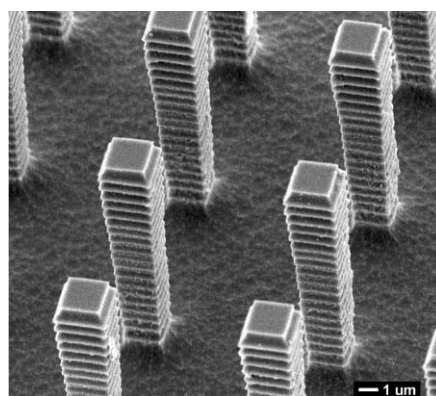


Fig. 1 Scanning electron microscope (SEM) image of bare silicon mesas upon which subsequent films were grown. The smallest of the arrays that were fabricated (having 2.5 × 2.5 µm faces) is shown.

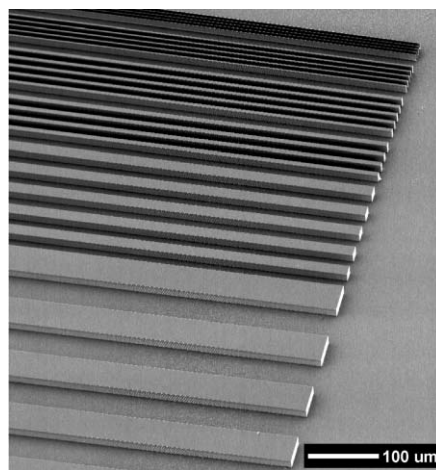


Fig. 2 Various sizes of bare silicon lines on silicon which were later deposited on to form channels that contained unique structures having sealed side walls and top faces.

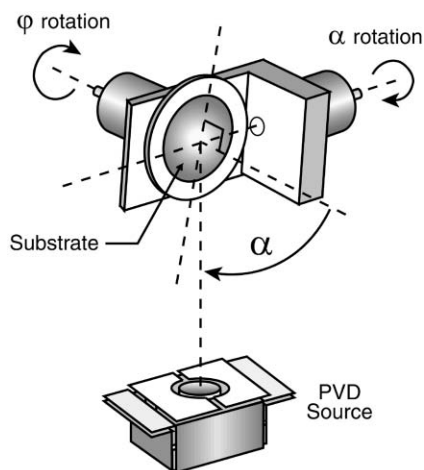


Fig. 3 Schematic illustration of the GLAD apparatus showing the range of substrate motion (ϕ and α rotation).

the diffusion length of the adatoms is limited, and the voided regions do not become filled. As the film further evolves, nanometer scale, columnar structures develop. Motion of the substrate during the deposition allows the growing nanocolumns to be engineered with a variety of possible morphologies.^{8–14} Deposition methods include thermal and electron beam evaporation, sputtering,¹⁴ and laser ablation techniques,¹¹ allowing an extensive range of materials to be grown.

The column density (related to the porosity of the film) is dependent on the incidence angle, α , with higher angles of incidence resulting in films with higher porosity (having wider spacing of the microstructures) and *vice versa*. The films can also be grown onto patterned or seeded substrates, where the microstructure density is enforced by the periodicity of the seeds. The size of the seeds then affects the resulting column sizes, with the column widths approaching the seed dimensions.¹⁵ Typically however, microstructures fabricated by the GLAD process are randomly distributed on the substrate, and all of the films grown on the Si mesas and channels shown here are as such.

Two different thin film microstructure types were grown on the arrays of Si mesas. One included oblique angle depositions that resulted in porous, slanted post films contained by solid walls along two edges of each mesa. The other was a helical film deposition that produced porous helices within sealed walls on all four edges of the mesas. Both film types were fabricated with silicon monoxide as a representative material, due to the ease of deposition and proven controllability of the microstructures on a scale of tens of nanometres.

For the oblique angle depositions, the corners of the mesas were aligned diagonal to the direction of incoming flux, which arrived at an incidence angle of 85° with respect to the substrate plane. A close-up view of one of the Si towers shows the solid border along two edges of the mesa (Fig. 4). Fig. 4 and 5 clearly show the shadowed regions that formed between the mesas. Solid walls can also be observed extending completely from the base to the top of the silicon up to the thickness of the film before curling slightly onto the top surface to meet with the porous region of the film. This resulted from an edge effect where the apparent incidence angle with respect to the perceived substrate at the corner changed abruptly from a few degrees along the vertical sides to 85° at the top face, thus causing the change from dense to porous film (Fig. 6). Standard, dense films are typically grown at zero or very low incidence angles, such that the flux arrives nearly perpendicular to the substrate. Therefore, whenever the flux approached a corner, the film would form a dense layer along the vertical side walls while forming a porous film on the top face; where the two met, a self-sealed wall would form. Changes in film

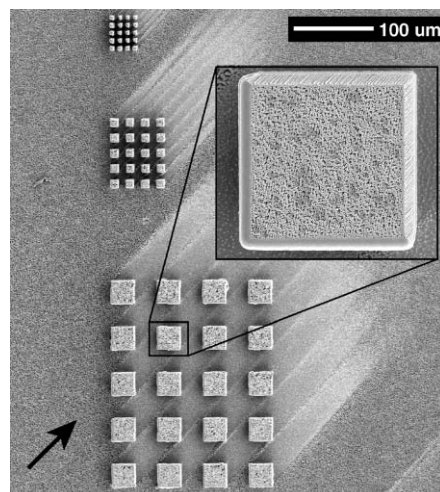


Fig. 4 Areal view of three arrays of mesas with GLAD-fabricated porous thin film grown on top. The thin film microstructures resemble slanted posts, and were grown by an oblique angle deposition, with the arrow indicating the direction of the vapour flux. One of the largest sized mesas is shown in the inset.

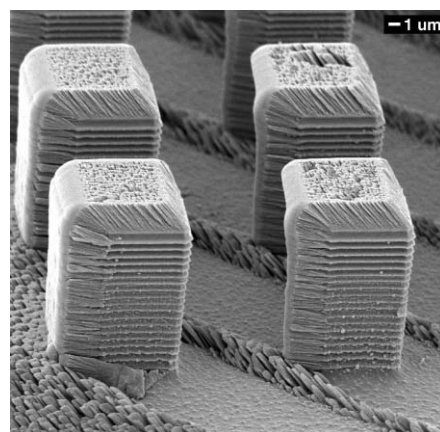


Fig. 5 Distinct shadowing is evident between the silicon mesas. Dense regions of film growth along the vertical Si sidewalls occurred for those facing the direction of arriving flux, while the top faces support a porous film.

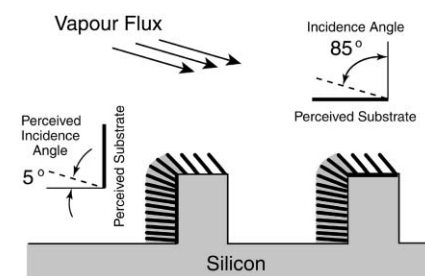


Fig. 6 Schematic illustration of the perceived substrate and perceived incidence angles as seen by the vapour flux as it encountered the sides and top faces of the mesas.

porosity have been demonstrated in capping layers⁷ (discussed later), where a porous film can be evolved into a dense layer that encapsulates the top surface of the film.

For the growth of helically structured films, the mesas were not aligned in any particular fashion, as rotation around the azimuthal direction, ϕ , disregards any prior arrangement of the substrate. Some of the helical films are shown in Fig. 7 and 8. As can be seen, a solid border completely encircles the porous regions for these films. Because the substrate was rotated

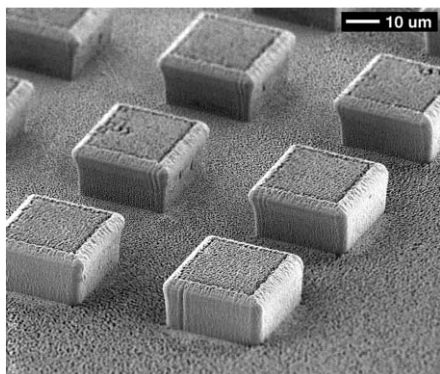


Fig. 7 Helically microstructured film deposition resulting in solid perimeters encircling each mesa. Surface debris is believed to have caused the irregularities seen on a few of the mesas.

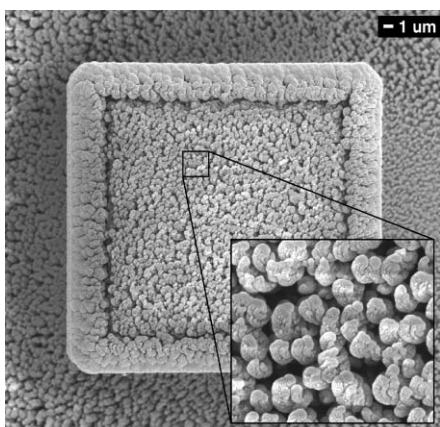


Fig. 8 Areal view of a microchamber showing the porous centre (with a close-up view in the inset) contained by a solid border.

completely around its axis to create helices with the desired number of turns, this resulted in “walls” that formed on all sides of the mesa, since flux was able to arrive from all directions. Average wall thicknesses were of the order of a few microns and, as a result, the smallest mesas did not produce a walled well structure containing a porous centre; the surface dimensions of the top face in comparison to the wall thickness were comparable, and therefore left no room for a porous region to form. The other mesas, however, were large enough to avoid this problem. Bifurcation of the structures that formed at the boundaries of the mesas (where the edge effect occurred) created these walls and hence reduced the area of the porous film region. Nevertheless, the vertical thickness of the film does have an affect on the thickness of the surrounding borders, so it would be conceivable to grow thinner films on the smallest mesas while still enabling porous regions to develop in the centres. The inner pore and channel sizes, therefore, have a dependency on the film thickness and on the amount of bifurcation of the walls.

Deposition of a capping layer over the helical microstructures allowed dense encapsulation layers to be grown over the films. This produced structures that consisted of porous thin film centres enclosed by solid walls on all sides. As the capping layer was deposited, the incidence angle ($\alpha = 85^\circ$) was dynamically reduced until it arrived at normal incidence ($\alpha = 0^\circ$). Fig. 9 shows some of the capped mesas, and Fig. 10 shows a cross-section of a Si line surmounted by a capped helical film. The latter figure reveals a microchannel with porous film encased by solid sidewalls and top capping layer that can be grown to any desired thickness to ensure complete encapsulation of the film underneath. Nano-indentation tests¹⁶ have shown that the pressure required to fracture a 200–300 nm

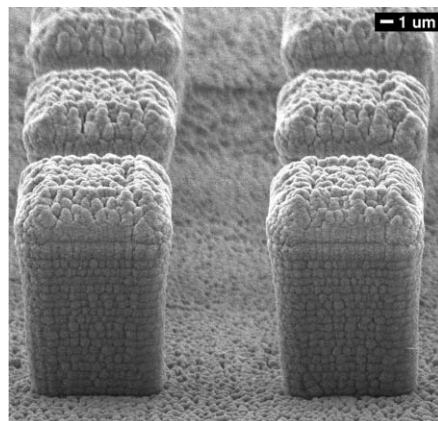


Fig. 9 Capped microchambers completely enclosed by encapsulation walls along all side and top faces.

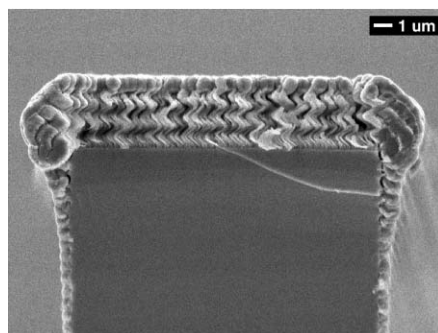


Fig. 10 Cross-sectional image of a capped helical film grown on a silicon line, forming a microchannel.

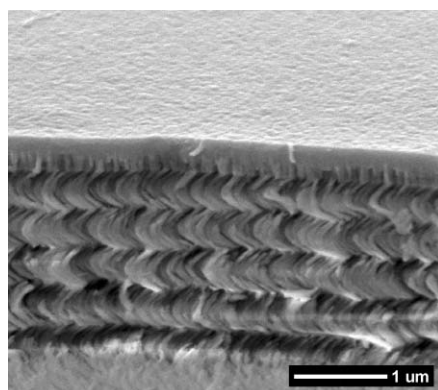


Fig. 11 A solid capping layer seals the top surface of the porous film.

thick SiO capping layer (Fig. 11) is approximately $1.25 \times 10^8 \text{ N m}^{-2}$ ($\sim 18\,000 \text{ psi}$), *i.e.* the layer is able to withstand the pressures (typically up to thousands of psi) found in some microfluidic systems¹⁷ and high pressure chromatographic systems.¹⁸

Discussion

The porous thin film centre within the solid walls of the microchamber compartments can be seen more closely in Fig. 8 and 11. The helical microstructures resemble a forest of “microsprings” whose geometry, thickness, and structure density can be modified during the deposition process. The unique nature of these highly porous films ($\sim 25\%$ of bulk density)¹⁹ is attractive for several reasons. Their extremely high surface area (tens to hundreds of times the spatial area of the sample substrate²⁰) may make them suitable for reactive or

catalytic applications if fabricated with the appropriate materials. Small pore sizes between the columnar structures can result in strong capillary effects, which could have potential applications for various types of sensors. A humidity sensor that was developed using these films possesses extremely rapid response times, due to the easy accessibility of the pores, which are anisotropic in nature.²¹ The physical characteristics of these films suggest possibilities for filtering, chromatographic, electrophoretic, or sensing applications. Other potential uses of these mesas may be in nano-assay applications, where several arrays of these chambers could be employed, requiring only a miniscule amount of reagent. Individual chambers could be utilized to carry out separate reactions, or an array of chemical sensors could be formed. Each reaction chamber or cell could also be individually addressed,²² scanned, and used with fluorescence detection systems, if grown on transparent glass substrates.²³

The ability to fabricate structures containing continuous walls sealing an interior of porous film could be applied to other shapes beyond the mesas and lines shown here. A raised pattern having edges where the vapour flux could encounter an abrupt change in substrate angle would result in the self-sealing edge effect. This attribute could be exploited with more complex shapes, such as T-junctions, so that a solid wall sealing a porous interior could be fabricated with almost any conceivable pattern.

Miniaturized reaction chambers are currently under development for lab-on-a-chip technology, which will bring the capabilities of expensive instruments to pocket-sized devices. The structures that have been fabricated here offer many possibilities that may lead to further developments in this field and others. At present, these structures are being studied to explore their potential applications.

References

1 T. Vo-Dinh and B. Cullum, *Fresenius' J. Anal. Chem.*, 2000, **366**, 540.

- 2 H. J. Lee, T. T. Goodrich and R. M. Corn, *Anal. Chem.*, 2001, **73**, 5525.
- 3 N. Maluf, *An Introduction to Microelectromechanical Systems*, Artech House, Boston, 2000, p. 66.
- 4 N. Maluf, *An Introduction to Microelectromechanical Systems*, Artech House, Boston, 2000, p. 51.
- 5 K. Robbie and M. J. Brett, *US Pat.*, 5866204, 1999.
- 6 K. Robbie, L. J. Friedrich, S. K. Dew, T. Smy and M. J. Brett, *J. Vac. Sci. Technol., A*, 1995, **13**, 1032.
- 7 K. Robbie and M. J. Brett, *J. Vac. Sci. Technol., A*, 1997, **15**, 1460.
- 8 K. Robbie, M. J. Brett and A. Lakhtakia, *J. Vac. Sci. Technol., A*, 1995, **13**, 2991.
- 9 K. Robbie, C. Shafai and M. J. Brett, *J. Mater. Res.*, 1999, **14**, 3158.
- 10 A. Lakhtakia, R. Messier, M. J. Brett and K. Robbie, *Innovations Mater. Res.*, 1996, **1**, 165.
- 11 D. Vick, Y. Y. Tsui, M. J. Brett and R. Fedosejevs, *Thin Solid Films*, 1999, **350**, 49.
- 12 R. Messier, T. Gehrke, C. Frankel, V. C. Venugopal, W. Otano and A. Lakhtakia, *J. Vac. Sci. Technol., A*, 1997, **15**, 2148.
- 13 S. R. Kennedy, M. J. Brett, O. Toader and S. John, *Nano Lett.*, 2002, **2**, 59.
- 14 J. C. Sit, D. Vick, K. Robbie and M. J. Brett, *J. Mater. Res.*, 1999, **14**, 1197.
- 15 B. Dick, M. J. Brett, T. J. Smy, M. R. Freeman, M. Malac and R. F. Egerton, *J. Vac. Sci. Technol., A*, 2000, **18**, 1838.
- 16 M. W. Seto, K. Robbie, D. Vick, M. J. Brett and L. Kuhn, *J. Vac. Sci. Technol., B*, 1999, **17**, 2172.
- 17 B. A. Buchholz, E. A. S. Doherty, M. N. Albarghouthi, F. M. Bogdan, J. M. Zahn and A. E. Barron, *Anal. Chem.*, 2001, **73**, 157.
- 18 H. Ahren, *The Scientist*, 1996, **10**(5), 17.
- 19 K. D. Harris, J. R. McBride, K. E. Nietering and M. J. Brett, *Sens. Mater.*, 2001, **13**, 225.
- 20 K. D. Harris, M. J. Brett, T. Smy and C. Backhouse, *J. Electrochem. Soc.*, 2000, **147**, 2002.
- 21 A. T. Wu, M. Seto and M. J. Brett, *Sens. Mater.*, 1999, **11**, 493.
- 22 P. Swanson, R. Gelbart, E. Atlas, L. Yang, T. Grogan, W. F. Butler, D. E. Ackley and E. Sheldon, *Sens. Actuators, B*, 2000, **64**, 22.
- 23 R. J. Lipshutz, S. P. A. Fodor, T. R. Gingeras and D. J. Lockhart, *Nature Genetics Suppl.*, 1999, **21**, 20.